J. Appl. Comput. Mech., 4(5) (2018) 467-481
DOI: 10.22055/JACM.2018.25161.1235

ISSN: 2383-4536
jacm.scu.ac.ir

M&MoCS

Shahid Chamran University of Ahvaz

Journal of Applied and Computational Mechanics

Research Paper

A General Rule for the Influence of Physical Damping on the Numerical Stability of Time Integration Analysis

Aram Soroushian

Structural Engineering Research Center, International Institute of Earthquake Engineering and Seismology, S. Lavasani (Farmaiyeh, North Dibajee, West Arghavan, No. 21,Tehran 19537, Iran

Received February 28 2018; Revised August 11 2018; Accepted for publication August 25 2018.
Corresponding author: Aram Soroushian, a.soroushian@iiees.ac.ir

Abstract. The influence of physical damping on the numerical stability of time integration analysis is an open question since decades ago. In this paper, it is shown that, under specific very general conditions, physical damping can be disregarded when studying the numerical stability. It is also shown that, provided the specific conditions are met, analysis of structural systems involved in extremely high linear-viscous damping is unconditionally stable. A secondary achievement is that, when the linear-viscous damping increases, the numerical damping may increase or decrease.

Keywords: Time integration, Numerical stability, Damping, Viscous, Numerical damping, Nonlinearity.

1. Introduction

Transient/dynamic behavior is an inherent part of almost all real phenomena, which cannot be simplified in many applications, e.g. analysis of tall buildings against severe wind or earthquake [1-3]. A powerful tool for analyzing these behaviors and in general initial value problems in different branches of science and engineering is time integration; see [4-18]. Concentrating on structural dynamics [12, 19, 20], the initial value problem defining the structural behavior is as stated below:

$$\begin{aligned} &\mathbf{M}\ddot{\mathbf{u}}(t)+\mathbf{f}_{\text{int}}(t)=\mathbf{f}(t) \quad , \quad 0\le t<t_{end} \\ &\mathbf{u}(t=0)=\mathbf{u}_0 \ , \ \dot{\mathbf{u}}(t=0)=\dot{\mathbf{u}}_0 \ , \ \mathbf{f}_{\text{int}}(t=0)=\mathbf{f}_{\text{int}_0} \\ &\mathbf{Q}\le\overline{\mathbf{O}} \end{aligned} \tag{1}$$

t and t_{end} imply the time and the duration of the dynamic behavior, $\mathbf{M}$ is the mass matrix, $\mathbf{f}_{\text{int}}(t)$ and $\mathbf{f}(t)$ stand for the vectors of internal force and excitation respectively, $\mathbf{u}(t)$, $\dot{\mathbf{u}}(t)$ and $\ddot{\mathbf{u}}(t)$ respectively denote the unknown vectors of displacement velocity and acceleration, $\mathbf{u}_0$, $\dot{\mathbf{u}}_0$ and $\mathbf{f}_{\text{int}_0}$ define the initial status of the system; also see [13, 21]; and $\mathbf{Q}\le\overline{\mathbf{O}}$ schematically represents the constraints considered additionally for modeling the nonlinear behaviors, e.g. impact or elastoplastic behavior; see [22, 23]). Solution of eq. (1) by time integration is summarized in Fig. 1; Subscripts 0 and i are indicators for the integration stations, respectively at the starting and arbitrary station of the integration, and Superscript a indicates that the argument is computed approximately.

The main algorithmic parameter of time integration analysis is the integration step Δt (see [24, 25]). Accordingly, the major essentiality of approximate computations, i.e. convergence [26, 27], can be expressed as:

$$\lim_{\Delta t\to 0}\upsilon^a=\upsilon \tag{2}$$

Published online November 25 2018

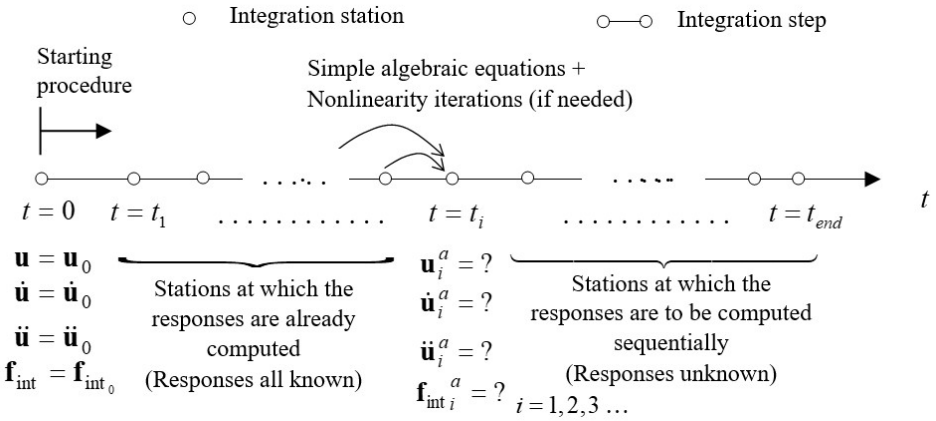

Fig. 1. Typical process of time integration analysis.

where, υ and υ^a respectively stand for the computed and exact values of the arbitrary component of the response. In view of the Lax-Richtmyer equivalence theorem [26-28], for the responses computed by time integration to converge, it is essential to guarantee numerical stability [27-31]. In more detail, in time integration analysis of a mathematically stable system (i.e. systems with finiteness guaranteed for all components of the exact response [32]; in structural dynamics, mathematical stability is equivalent to physical stability [13]), for maintaining responses convergence, the computation should be consistent (i.e. in analysis with smaller steps, the errors associated with arbitrary integration step should decrease faster than the integration step [31, 33]) and numerically stable. Numerical stability can be defined by [31, 33]:

$$\forall \text{ Finite initial conditions and } \forall \text{ Finite excitation} \Rightarrow \forall \upsilon^a : \left\|\upsilon^a\right\| < \infty \cdot \tag{3}$$

Numerical stability and convergence imply the capability to avoid uncontrollable large computational errors regardless of the number and size of the integration steps. These features are important and essential because of two main reasons. First, in order to guarantee finite inaccuracy (controllable accuracy) after arbitrarily large number of steps in applications such as meteorological and astrophysical studies [6, 7, 34], and secondly, for controlling the accuracy by repeating the analysis with smaller steps, obligatory in applications such as earthquake engineering [19, 35]. Furthermore, it is decades, that unconditional stability, i.e. numerical stability regardless of the integration step, is a privilege when defining new integration methods [12, 20, 31, 33, 36]. The crucial role of stability in some specific linear and nonlinear applications is reported in [37-43].

In order to study the validity of eq. (3) and guarantee responses' numerical stability, it is conventional to first assume

$$\begin{aligned} \mathbf{f}_{\text{int}} &= \mathbf{K}\mathbf{u} + \mathbf{C}\dot{\mathbf{u}} \\ \mathbf{C} &= \mu\mathbf{M} + \lambda\mathbf{K} \end{aligned} \tag{4}$$

(**K** is the linear stiffness matrix, **C** implies the linear-viscous damping matrix, and μ and λ are constant coefficients, indicating that the linear-viscous damping is classical and of the Rayleigh type [12, 19, 20, 44]). Under this assumption, for the study of numerical stability, it is necessary and sufficient to study the arbitrary linear SDOF (Single Degree Of Freedom) system below:

$$\ddot{u} + 2\xi\omega\dot{u} + \omega^2 u = 0 \tag{5}$$

(ξ is the coefficient of the linear-viscous damping, and ω, m, $c = 2\xi\omega m$, and $k = \omega^2 m$, stand for the natural frequency, mass, linear-viscous damping, and linear stiffness, respectively [19]), construct the amplification matrix, **A**, as:

$$\begin{pmatrix} u^a \\ \dot{u}^a \Delta t \\ \ddot{u}^a \Delta t^2 \end{pmatrix}_i = \mathbf{A} \begin{pmatrix} u^a \\ \dot{u}^a \Delta t \\ \ddot{u}^a \Delta t^2 \end{pmatrix}_{i-1} \quad , \quad i = 1,2,3,\ldots \tag{6}$$

and test the spectral radius of **A**, i.e. $\rho(\mathbf{A})$ [45] for the validity of eq. (7):

$$\rho(\mathbf{A}) \le 1 \quad \text{or} \quad \rho(\mathrm{A}) < 1 \tag{7}$$

depending on whether one or more eigen values of **A** equal $\rho(\mathbf{A})$ [33]. (For some integration methods, e.g. the Houbolt method [46], higher time derivatives exist in eq. (6); this does not affect the discussion in this paper.) Satisfaction of eq. (7) entails numerical stability [12, 13, 31, 33].

For MDOF (Multi Degree Of Freedom) systems, the discussion above can be valid also without the assumption of classical damping, if eq. (6) is re-defined for the total system [47, 48]. When the damping is classical, the linear behavior of the MDOF system can be represented by SDOF systems [12, 20, 31, 33, 47]. Accordingly, in order to study the stability of a specific integration scheme, it is essential to consider eqs. (5-7) and obtain ρ for different values of ω, Δt, and ξ. In more detail, for the study of stability, one should compute the amplification matrix for different values of $\omega\Delta t$ and ξ, and for each computation of the amplification matrix the spectral radius should be determined. The resulting spectral radii will lead to Fig. 2 and the study of eq. (7).

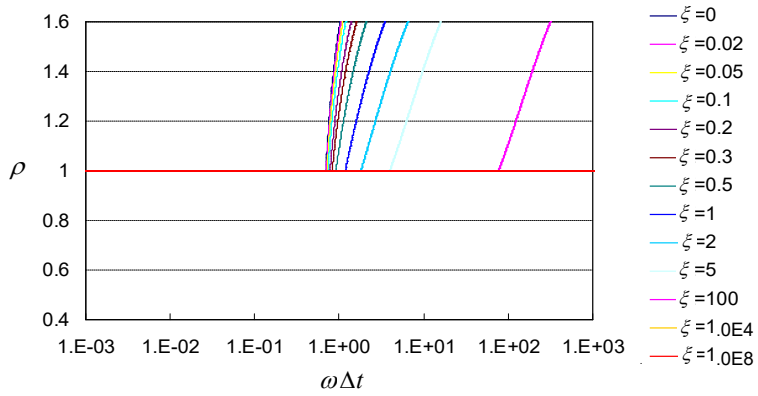

Fig. 2. Typical changes of spectral radius versus $\omega\Delta t$ in conventional study of numerical stability.

If under specific conditions, linear-viscous damping can be reliably beneficial for numerical stability, it will be possible to study the stability, after disregarding the damping. To say better, if a rule can be found to guarantee enhancement of numerical stability of time integration analysis when adding the linear-viscous damping, instead of studying the validity of eq. (7), i.e.

$$\rho(\mathbf{A}) = g(\omega\Delta t, \xi) \not> 1 \qquad \text{or} \qquad \rho(\mathbf{A}) = g(\omega\Delta t, \xi) \not\geq 1 \tag{8}$$

it will be sufficient to study the simpler requirement below:

$$\rho(\mathbf{A}) = g(\omega\Delta t, \xi = 0) \not> 1 \qquad \text{or} \qquad \rho(\mathbf{A}) = g(\omega\Delta t, \xi = 0) \not\geq 1 \tag{9}$$

This implies the sufficiency of studying Fig. 3, instead of Fig. 2. Such studies are not addressed in the literature, e.g. see [12, 13, 20, 29, 31, 33, 43, 49-57]. The only study on the issue, mainly stating that the effect of damping on numerical stability depends on different conditions (not stated in the report of the study), returns to 1987 [58]. Considering this, the more ease and less computational effort associated with Fig. 3 compared to Fig. 2, and the crucial role of numerical stability in real analyses [37-42], the objective of this paper is to develop a rule, that clarifies the influence of physical damping on the numerical stability. Generalization of the achievements from viscous damping to other types of damping is also under attention. The theory is explained first. Validity of the claims is discussed later, and the discussion is extended afterwards. The paper is concluded, with a brief set of the achievements.

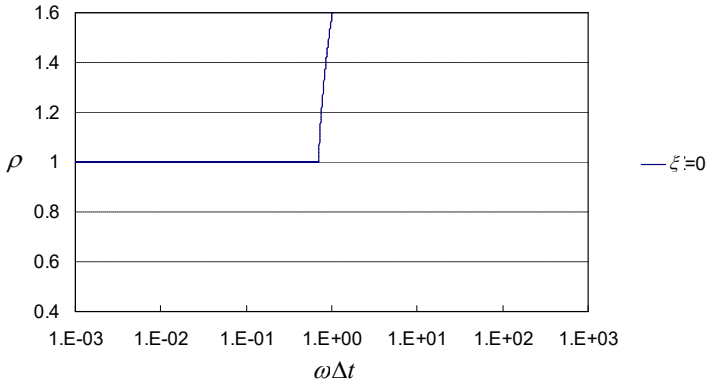

Fig. 3. Simplified study of Fig. 2 to be validated in this paper.

2. Theory

With attention to Fig. 1, the definition of numerical stability in eq. (3), and eq. (6), an arbitrary unstable response does not become infinitely large, from the starting steps of the analysis. Figure 4 displays this phenomenon and some examples are presented in [59]. To explain better, consider the extension of eq. (6), to forced vibration of MDOF system [12, 20, 33, 36, 47], stated below:

$$\begin{pmatrix} \mathbf{u}^a \\ \dot{\mathbf{u}}^a \Delta t \\ \ddot{\mathbf{u}}^a \Delta t^2 \end{pmatrix}_n = \mathbf{A} \begin{pmatrix} \mathbf{u}^a \\ \dot{\mathbf{u}}^a \Delta t \\ \ddot{\mathbf{u}}^a \Delta t^2 \end{pmatrix}_{n-1} + \mathbf{L} \begin{pmatrix} \mathbf{f}_{n-1} \\ \mathbf{f}_n \end{pmatrix} \qquad , \qquad n = 1,2,3,\ldots \tag{10}$$

(**L** stands for the load operator, and n implies the step under consideration, equivalently equal to the number of the integration steps prior to the step under consideration.) By replacing the computed values with the exact values, eq. (10) changes form to

$$\begin{pmatrix} \mathbf{u} \\ \dot{\mathbf{u}} \Delta t \\ \ddot{\mathbf{u}} \Delta t^2 \end{pmatrix}_n = \mathbf{A} \begin{pmatrix} \mathbf{u} \\ \dot{\mathbf{u}} \Delta t \\ \ddot{\mathbf{u}} \Delta t^2 \end{pmatrix}_{n-1} + \mathbf{L} \begin{pmatrix} \mathbf{f}_{n-1} \\ \mathbf{f}_n \end{pmatrix} - \tau_n \qquad , \qquad n = 1,2,3,\ldots \tag{11}$$

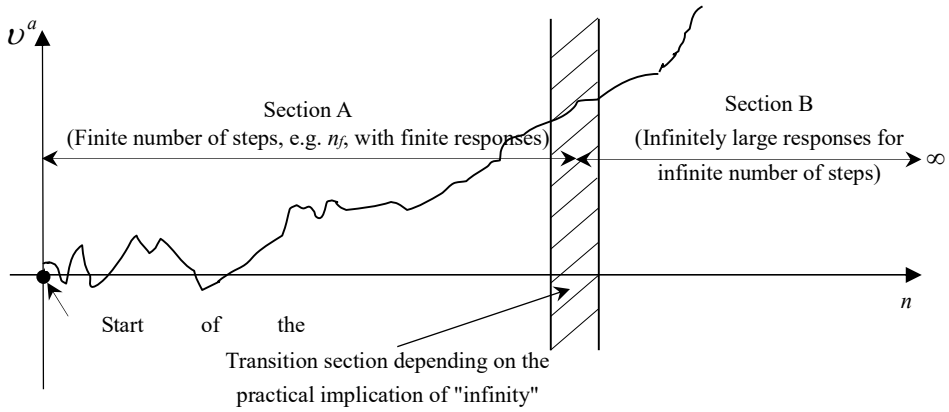

Fig. 4. Schematic illustration of an arbitrary unstable response obtained from time integration analysis.

where, τ_n is a representative of the difference between the computed and exact responses at the n th station, considering no difference at the n-1 th station, i.e.

$$\tau_n = \begin{pmatrix} \mathbf{u}^a \\ \dot{\mathbf{u}}^a \Delta t \\ \ddot{\mathbf{u}}^a \Delta t^2 \end{pmatrix}_n - \begin{pmatrix} \mathbf{u} \\ \dot{\mathbf{u}} \Delta t \\ \ddot{\mathbf{u}} \Delta t^2 \end{pmatrix}_n \quad \textbf{provided:} \quad \begin{pmatrix} \mathbf{u}^a \\ \dot{\mathbf{u}}^a \Delta t \\ \ddot{\mathbf{u}}^a \Delta t^2 \end{pmatrix}_{n-1} = \begin{pmatrix} \mathbf{u} \\ \dot{\mathbf{u}} \Delta t \\ \ddot{\mathbf{u}} \Delta t^2 \end{pmatrix}_{n-1} \tag{12}$$

Equations (10-12) lead to (see [33]):

$$\begin{pmatrix} \mathbf{u}^a \\ \dot{\mathbf{u}}^a \Delta t \\ \ddot{\mathbf{u}}^a \Delta t^2 \end{pmatrix}_n = \mathbf{A}^n \begin{pmatrix} \mathbf{u}_0 \\ \dot{\mathbf{u}}_0 \Delta t \\ \ddot{\mathbf{u}}_0 \Delta t^2 \end{pmatrix} + \sum_{k=1}^{n} \mathbf{A}^{n-k} \mathbf{L} \begin{pmatrix} \mathbf{f}_{k-1} \\ \mathbf{f}_k \end{pmatrix} \quad , \quad n = 1,2,3,\ldots \tag{13.1}$$

$$\begin{pmatrix} \mathbf{u}^a \\ \dot{\mathbf{u}}^a \Delta t \\ \ddot{\mathbf{u}}^a \Delta t^2 \end{pmatrix}_n - \begin{pmatrix} \mathbf{u} \\ \dot{\mathbf{u}} \Delta t \\ \ddot{\mathbf{u}} \Delta t^2 \end{pmatrix}_n = \mathbf{A}^{n-1}\tau_1 + \mathbf{A}^{n-2}\tau_2 + \ldots + \mathbf{A}^2\tau_{n-2} + \mathbf{A}\tau_{n-1} + \tau_n = \sum_{k=0}^{n-1} \mathbf{A}^k \tau_{n-k} \tag{13.2}$$

$$\left\| \begin{pmatrix} \mathbf{u}^a \\ \dot{\mathbf{u}}^a \Delta t \\ \ddot{\mathbf{u}}^a \Delta t^2 \end{pmatrix}_n - \begin{pmatrix} \mathbf{u} \\ \dot{\mathbf{u}} \Delta t \\ \ddot{\mathbf{u}} \Delta t^2 \end{pmatrix}_n \right\| \le \sum_{k=0}^{n-1} \|\mathbf{A}\|^k \, \|\tau_{n-k}\| \tag{13.3}$$

where, $\|\tau_k\|$ equals the local truncation error [31, 33, 60], and in arriving at eq. (13.2), mathematical induction [61] is implemented. In view of eqs. (12) and (13.3), and the role of spectral radius in the size of $\mathbf{A}$, i.e. $\|\mathbf{A}\|$ [12, 20, 31, 33, 36], the unstable responses cannot be infinitely large, when n is sufficiently small; see Fig. 4 and [59]. Therefore, although there is not a clear separation between Sections A and B in Fig. 4,

$$n_f > 0 \tag{14}$$

In view of Fig. 4, eq. (14) might seem incorrect, when the natural frequencies of the system are extremely high. This is not true. The highly oscillatory natural modes generally are erroneously added to the mathematical model during spatial discretization [36, 62]; elimination of these unreal oscillations is essential [12, 20, 33, 36]. In the rare cases that these oscillations originate in the real behavior, accuracy considerations bound Δt [12, 13, 19], and again eq. (14) holds.

Based on Fig. 4 and the explanation above, for the starting n_f integration steps of an unstable analysis,

$$\forall\, \upsilon^a \text{ defined for the starting } n_f \text{ steps:} \quad \|\upsilon^a\| < \infty \quad , \quad \lim_{\Delta t \to 0} \upsilon^a \neq \upsilon \tag{15}$$

The last part of eq. (15) is concluded from the instability of the response and the Lax-Richtmyer theorem [26-28], taking into account the consistency, as an assumption. Equations (14) and (15) are obtained for arbitrary unstable response. In continuation of this section, it is shown that, provided special conditions are satisfied, eqs. (14) and (15) cannot both be correct, when time integration analysis of the associated undamped system (similar mass, stiffness, excitation, and initial conditions) with the same integration method and step is numerically stable.

As conventional in the study of numerical stability [31, 33], attention here is paid to the damped SDOF system below:

$$\begin{aligned} &m\ddot{u} + c\dot{u} + ku = f(t) \quad , \quad 0 \le t < t_{end} \\ &u(t=0) = u_0 \ , \ \dot{u}(t=0) = \dot{u}_0 \end{aligned} \tag{16}$$

where,

$$c \neq 0 \tag{17}$$

It is meanwhile assumed that the time integration method is consistent, and the analysis of the associated undamped system, i.e.

$$\begin{aligned} &m\ddot{u}+ku=f\left(t\right) \quad , \quad 0\le t<t_{end} \\ &u\left(t=0\right)=u_0 \ , \ \dot{u}\left(t=0\right)=\dot{u}_0 \end{aligned} \tag{18}$$

is numerically stable, i.e. in view of eq. (3),

$$\left\|\upsilon_{und}^{a}\right\|<\infty \tag{19}$$

where, υ_{und}^{a} represents an arbitrary response computed for eq. (18). Addressing the responses obtained for eq. (16) as υ_{damp}^{a}, the stability of υ_{damp}^{a} is to be shown.

Assume that υ_{damp}^{a} is unstable. In view of Fig. 4 and eqs. (14) and (15), the computed unstable response remains finite for few steps after the start of the analysis. Accordingly, u_{damp}^{a}, $\dot{u}_{damp}^{a}$, and $\ddot{u}_{damp}^{a}$, remain finite at n_f non-zero number of steps at the start of the analysis. Because of this finiteness, it is possible to define the system below:

$$\begin{aligned} &m\ddot{u}+ku=f\left(t\right)-\kappa c\dot{u}_{damp}^{a} \quad , \quad 0\le t<t'_{end} \\ &u\left(t=0\right)=u_0 \\ &\dot{u}\left(t=0\right)=\dot{u}_0 \end{aligned} \tag{20}$$

where, κ implies an arbitrary real number and t'_{end} is obtainable from:

$$0<t'_{end}=n_l\Delta t<\infty \quad , \quad 0<n_l\le n_f \tag{21}$$

Responses computed for the problems in eqs. (16) and (20) can be identical. In more detail, provided using the integration method and the integration step used in obtaining $\dot{u}_{damp}^{a}$, in analysis of eqs. (16) and (20), the resulting two responses will be identical, when in the integration formulation the equations involved in the excitation have contributions from damping, and the contributions associated with damping and excitation can be canceled out by appropriate selection of κ. Selection of the appropriate value for κ will be possible, specifically when both or none of the damping and the excitation exists in each equation defining the integration scheme. Many time integration methods satisfy this condition, e.g. see Table 1. By considering:

- that the responses computed for eqs. (16) and (20) are identical at $0\le t<t'_{end}$,
- the fact that eq. (20) presents an undamped problem, and
- that the integration method provides numerically stable responses for undamped problems,

Table 1. Adequate values for κ in eq. (20) for some time integration methods.

Method	Scheme	κ
Three-step Houbolt [46]	$m\ddot{u}_n+c\dot{u}_n+ku_n=f_n$ $\dot{u}_n=\frac{1}{6\Delta t}\left(11u_n-18u_{n-1}+9u_{n-2}-2u_{n-3}\right)$ $\ddot{u}_n=\Delta t^{-2}\left(2u_n-5u_{n-1}+4u_{n-2}-u_{n-3}\right)$	1
Newmark [63]	$m\ddot{u}_n+c\dot{u}_n+ku_n=f_n$ $\dot{u}_n=\dot{u}_{n-1}+\left[\left(1-\gamma\right)\Delta t\right]\ddot{u}_{n-1}+\left(\gamma\Delta t\right)\ddot{u}_n$ $u_n=u_{n-1}+\Delta t\dot{u}_{n-1}+\left[\left(0.5-\beta\right)\Delta t^2\right]\ddot{u}_{n-1}+\left(\beta\Delta t^2\right)\ddot{u}_n$	1
Central difference [64]	$m\ddot{u}_{n-1}+c\dot{u}_{n-1}+ku_{n-1}=f_{n-1}$ $\dot{u}_{n-1}=0.5\Delta t^{-1}\left(u_n-u_{n-2}\right)$ $\ddot{u}_{n-1}=\Delta t^{-2}\left(u_n-2u_{n-1}+u_{n-2}\right)$	1
C-H [65]	$m\ddot{u}_{n-\alpha_m}+c\dot{u}_{n-\alpha_f}+ku_{n-\alpha_f}=f\left(t_{n-\alpha_f}\right)$ $\dot{u}_n=\dot{u}_{n-1}+\left[\left(1-\gamma\right)\Delta t\right]\ddot{u}_{n-1}+\left(\gamma\Delta t\right)\ddot{u}_n$ $u_n=u_{n-1}+\Delta t\dot{u}_{n-1}+\left[\left(0.5-\beta\right)\Delta t^2\right]\ddot{u}_{n-1}+\left(\beta\Delta t^2\right)\ddot{u}_n$ $\ddot{u}_{n-\alpha_m}=\left(1-\alpha_m\right)\ddot{u}_n+\alpha_m\ddot{u}_{n-1}$ $\dot{u}_{n-\alpha_f}=\left(1-\alpha_f\right)\dot{u}_n+\alpha_f\dot{u}_{n-1}$ $u_{n-\alpha_f}=\left(1-\alpha_f\right)u_n+\alpha_f u_{n-1}$ $\gamma=0.5-\alpha_m+\alpha_f \quad , \quad \beta=0.25\left(1-\alpha_m+\alpha_f\right)^2$ $\alpha_m=\left(2\rho_\infty-1\right)/\left(\rho_\infty+1\right) \quad , \quad \alpha_f=\rho_\infty/\left(\rho_\infty+1\right)$	$\frac{\dot{u}\left(t_{n-\alpha_f}\right)}{\dot{u}_{n-\alpha_f}}$

the existence of an appropriate value for κ implies stability of the responses computed for eq. (16). As a consequence, the assumption of the instability of υ^{a}_{damp} and the last relation in eq. (15) are incorrect. In other words, the responses computed for the damped problem are stable. Therefore, when:

- The damping is linear-viscous.
- The damping and the excitation contribute the integration scheme, such that a value can be assigned to κ entailing identical responses for eqs. (16) and (20), when time integrated with the similar integration step.
- The integration method is consistent.

numerical stability of the undamped system's analysis implies the stability of the associated linear-viscous damped systems' analyses. For further reliability and clarity of the discussion on the notion of finiteness, the structural system is considered physicallystable, when undamped; see [59]. Hence, when: (a) the time integration scheme is consistent, (b) the damping is linear-viscous, (c) the damping contributes in the integration scheme, such that eqs. (16) and (20) can lead to identical responses when time integrated with the same integration step, and (d) the structural system is physically stable, numerical stability of the undamped system's analysis implies numerical stability of the associated damped systems' analyses. This conclusion entails Fig. 5 (ω is the oscillatory frequency, in many cases that of the highest natural mode), according to which, for arbitrary time integration method, when the above-mentioned four conditions are satisfied,

- The range of values of $\omega\Delta t$ resulting in unstable responses for linear-viscous damped analyses will be a subset of the range of values of $\omega\Delta t$ resulting in unstable responses for the associated undamped analysis.
- Equivalently, the range of $\omega\Delta t$ resulting in stable responses for an undamped analysis will be a subset of the range of $\omega\Delta t$ resulting in stable responses for the associated linear-viscous damped analyses.
- Unconditional instability may turn to stability or even unconditional stability by adding linear-viscous damping.
- Stability of an undamped system's time integration analysis will imply stability of the associated linear-viscous damped systems' analyses.

In analysis of MDOF systems, for the validity of the above claims, besides Conditions (a)-(d), the damping should be classical; see the extension in Section 4. For nonlinear analyses, Conditions (a)-(d) are necessary; see Section 5.

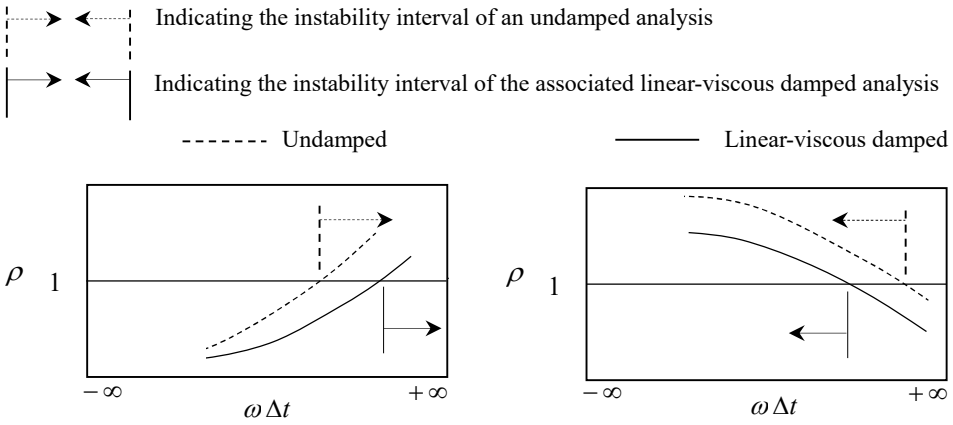

Fig. 5. Effect of linear-viscous damping on spectral radius when Conditions (a)-(d) are met.

3. Numerical Illustration

In this section, the validity of Fig. 5 is studied via different conventional and recent time integration methods [19, 46, 63-72]. First, it is displayed that when Conditions (a)-(d) addressed in Section 2 are provided, linear-viscous damping is beneficial for numerical stability; see Figs. 6-18, where

$$T = 2\pi\omega^{-1} \tag{22}$$

and the values of ξ are selected from:

$$\xi = 0,.02,0.05,0.1,0.5,1,2,100,10^{4},10^{8} \tag{23}$$

Extremely large values of ξ are considered in eq. (23), in order to clarify any probable ambiguity regarding the effects of large damping on numerical stability. Obviously, Figs. 6-18 are in complete agreement with Fig. 5 (see [19, 46, 63-71] and consider physical stability for the system under consideration).

Then, the importance and role of Condition (c) (stated in Section 2) in the validity of Fig. 5 is studied via an integration method recently proposed by Rezaiee-Pajand and Karimi-Rad [72]. As apparent in Fig. 19 and Table 2, when using this integration method, linear-viscous damping is not necessarily beneficial for the numerical stability (Δt_{cr} is the largest integration step leading to numerical stability, roughly speaking equal to the integration step in Figs. 2, 3, and 5, at which, the spectral radius increases from values smaller than one to values larger than one). Nevertheless, this is not against the claims made in Section 2 and Fig. 5; see the formulation of this method [72], stated below:

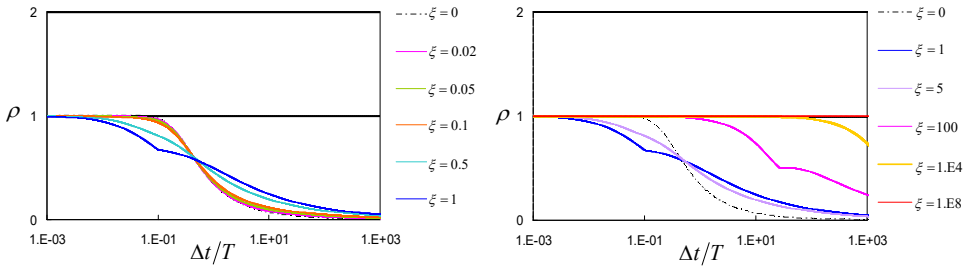

(a) (b)

Fig. 6. Changes of spectral radius with respect to $\Delta t/T$ for the Houbolt method [46]: (a) low ξ, (b) high ξ.

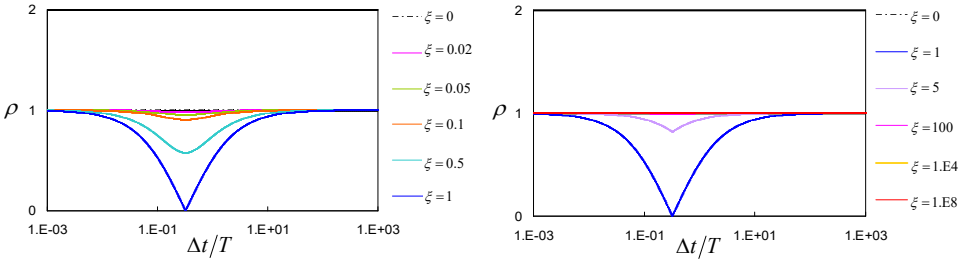

(a) (b)

Fig. 7. Changes of spectral radius with respect to $\Delta t/T$ for the Newmark average acceleration method [63]: (a) low ξ, (b) high ξ.

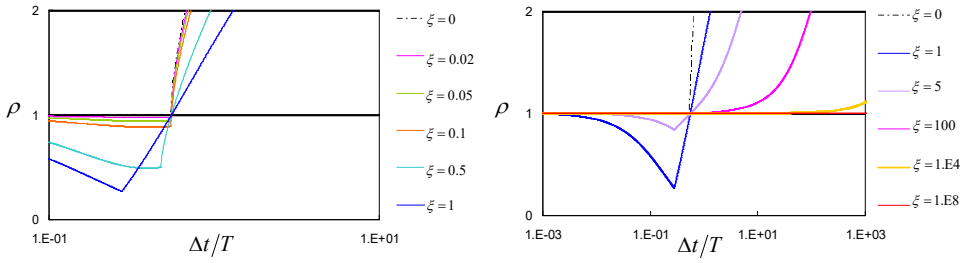

(a) (b)

Fig. 8. Changes of spectral radius with respect to $\Delta t/T$ for the Newmark linear acceleration method [19]: (a) low ξ, (b) high ξ.

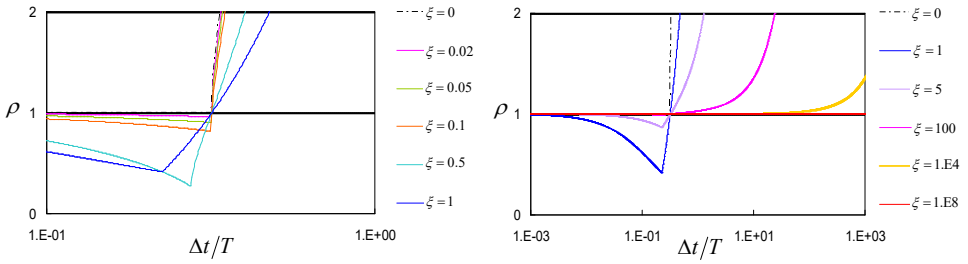

(a) (b)

Fig. 9. Changes of spectral radius with respect to $\Delta t/T$ for the central difference method [64]: (a) low ξ, (b) high ξ.

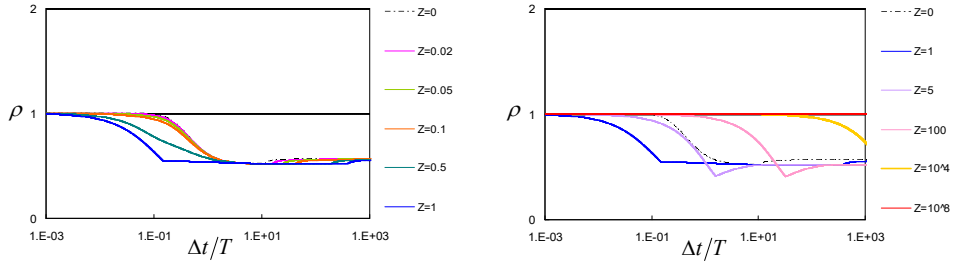

(a) (b)

Fig. 10. Changes of spectral radius with respect to $\Delta t/T$ for the Wilson-Theta method ($\theta = 1.42$) [66]: (a) low ξ, (b) high ξ.

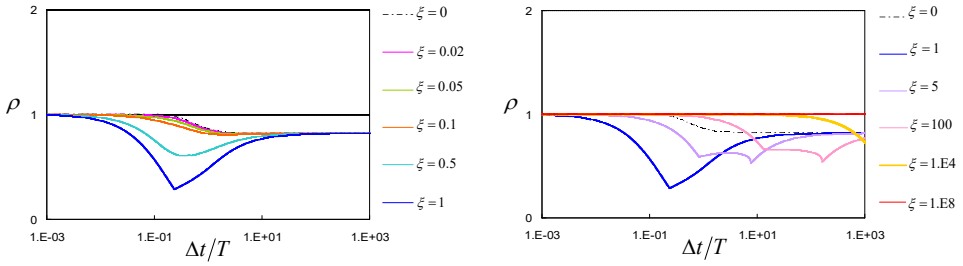

(a) (b)

Fig. 11. Changes of spectral radius with respect to $\Delta t/T$ for the HHT method [67] ($\alpha = -0.1$, $\beta = 0.3025$, $\gamma = 0.6$): (a) low ξ, (b) high ξ.

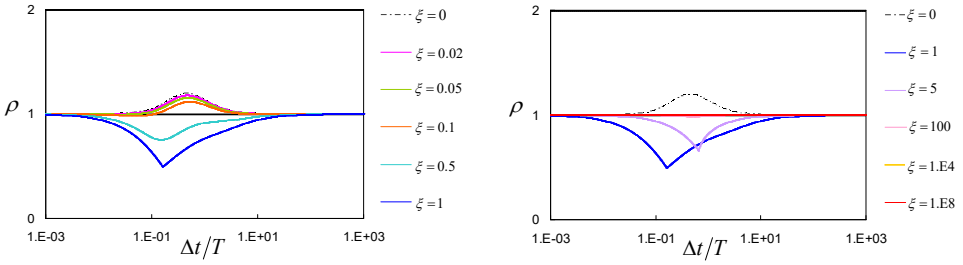

(a) (b)

Fig. 12. Changes of spectral radius with respect to $\Delta t/T$ for the HHT method [67] ($\alpha = -0.3$, $\beta = 0.25$, $\gamma = 0.5$): (a) low ξ, (b) high ξ.

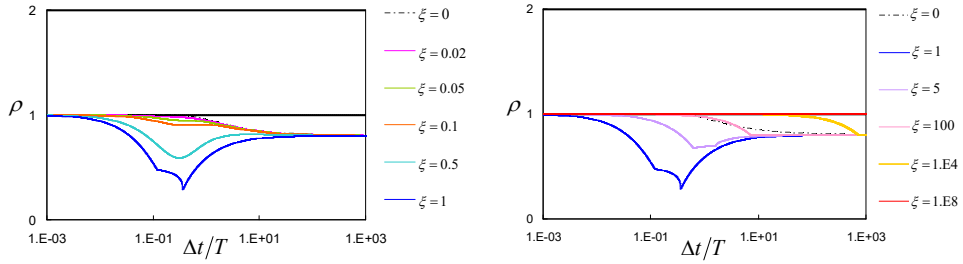

(a) (b)

Fig. 13. Changes of spectral radius with respect to $\Delta t/T$ for the C-H method ($\rho_\infty = 0.8$) [65]: (a) low ξ, (b) high ξ.

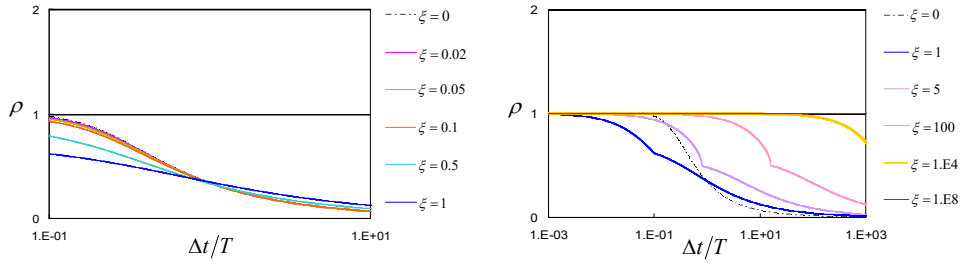

(a) (b)

Fig. 14. Changes of spectral radius with respect to $\Delta t/T$ for the C-H method ($\rho_\infty = 0$) [65]: (a) low ξ, (b) high ξ.

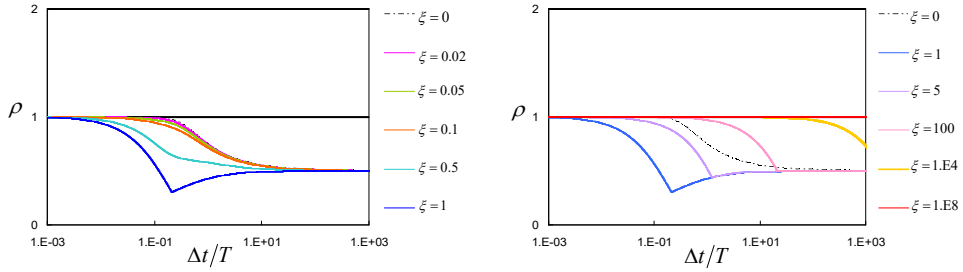

(a) (b)

Fig. 15. Changes of spectral radius with respect to $\Delta t/T$ for the C-H method ($\rho_\infty = 0.5$) [65]: (a) low ξ, (b) high ξ.

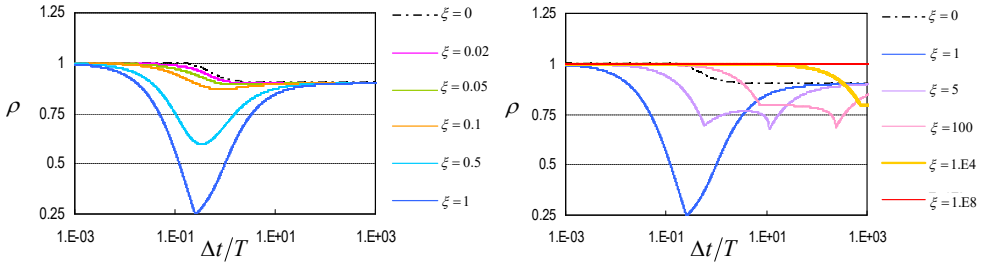

Fig. 16. Changes of spectral radius with respect to $\Delta t/T$ for the θ_1 method ($\theta_1 = 0.975$) [68]: (a) low ξ, (b) high ξ.

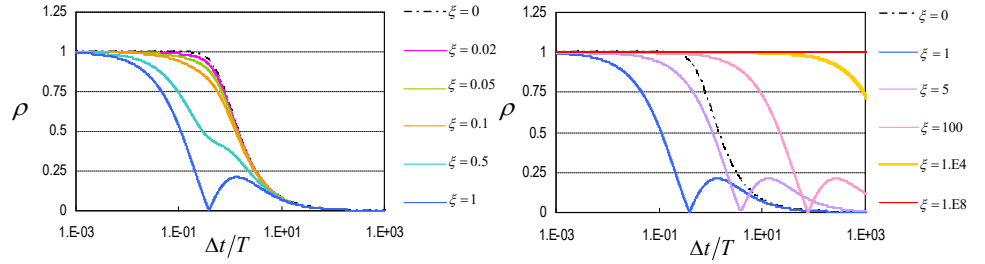

Fig. 17. Changes of spectral radius with respect to $\Delta t/T$ for the method of Bathe [69, 70]: (a) low ξ, (b) high ξ.

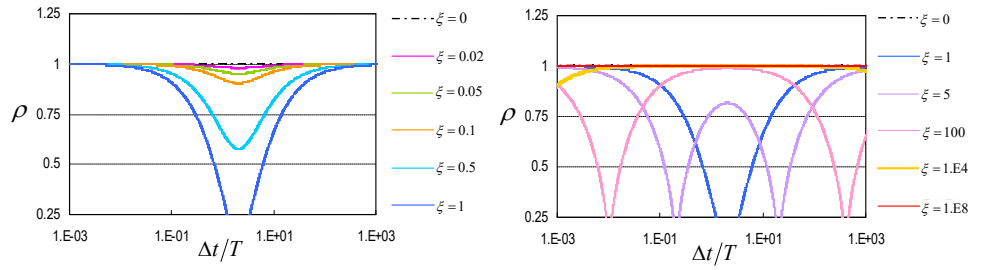

Fig. 18. Changes of spectral radius with respect to $\Delta t/T$ for the method of Katsikadelis [71]: (a) low ξ, (b) high ξ.

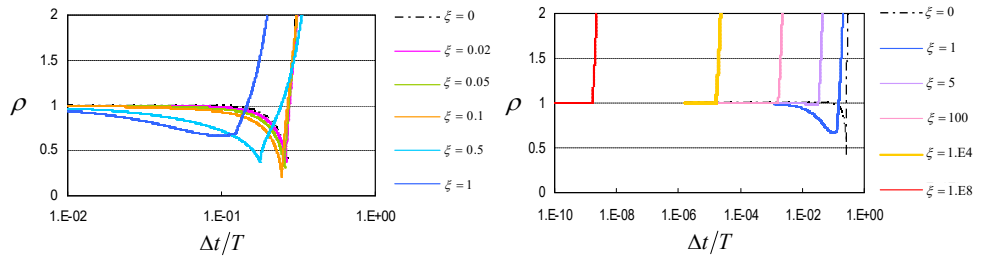

Fig. 19. Changes of spectral radius with respect to $\Delta t/T$ for the method of Rezaiee Pajand and Karimi-Rad ($\alpha = 0.9$) [72]: (a) low ξ, (b) high ξ.

$$
\begin{aligned}
&\bar{u}_n = u_n + 0.5\,\Delta t\,\dot{u}_n \\
&\bar{\dot{u}}_n = \dot{u}_n + 0.5\,\Delta t\,\ddot{u}_n \\
&\bar{f}_n = 0.5\left(f_n + f_{n+1}\right) \\
&m\bar{\ddot{u}}_n + c\,\bar{\dot{u}}_n + k\,\bar{u}_n = \bar{f}_n \\
&\dot{u}_{n+1} = u_n + \Delta t\,\bar{\ddot{u}}_n \\
&\hat{u}_n = u_n + 0.5\Delta t\,\dot{u}_n + 0.25\alpha^{-1}\Delta t^2\,\bar{\ddot{u}}_n + 0.125\,\alpha^{-1}\left(\alpha - 2\right)\Delta t^2\,\ddot{u}_n \\
&u_{n+1} = \frac{4}{3}\hat{u}_n - \frac{1}{3}u_n + \frac{\Delta t}{3}\dot{u}_{n+1} \\
&m\,\ddot{u}_{n+1} + c\,\dot{u}_{n+1} + k\,u_{n+1} = f_{n+1} \\
&\alpha > 0.4
\end{aligned}
\tag{24}
$$

and consider that the κ introduced in Section 2 cannot exist for the scheme in eq. (24). Consequently, Figs. 6-19 are in complete agreement with Fig. 5, as well as the study reported in [58].

Table 2. Changes of $\Delta t_{cr}/T$ with respect to ξ for the method proposed in [72] ($\alpha = 0.9$).

ξ	0	0.02	0.05	0.10	0.50	1	5	100	1E4	1E8
$\Delta t_{cr}/T$	0.2781	0.2756	0.2720	0.2675	0.2429	0.1456	0.08425	0.03638	0.159E-4	0.159E-8

In addition, in Figs. 6-18,

$$\forall\ \omega\Delta t: \quad \lim_{\xi \to \infty} \rho = 1 \tag{25}$$

This observation can be explained, by the fact that, at $\xi \to \infty$ the behavior is asymptotically static, and hence, for the actual (exact) response,

$$\xi \to \infty: \quad \dot{u} \to 0 \quad \text{and} \quad \ddot{u} \to 0 \tag{26}$$

Besides, the Conditions (a)-(d) stated in Section 2 are considered satisfied in Figs. 6-18. Therefore, in agreement with the achievements in Section 2, at $\xi \to \infty$, regardless of the integration step, the computed responses are both consistent and stable. The consequence is responses convergence to the actual responses. Accordingly, eq. (26) implies $\rho = 1$ regardless of the integration step. This is an evidence for the validity of eq. (25). When, the Conditions (a)-(d) are not satisfied, although eq. (26) will remain correct, eq. (25) is not necessarily correct, because of the lack of guarantee on stability and convergence. Figure 19 displays an example. (Meanwhile, eq. 25 can be explained also with attention to the geometry of Fig. 5.)

Furthermore, as apparent in Figs. 6-19, the changes of spectral radius with respect to viscous damping do not occur in a monotone trend for different values of $\Delta t/T$. In more detail, for unconditionally stable analyses, the trends of the changes of ρ with respect to $\Delta t/T$ are different before and after about $\xi = 1$ (associated with the critically damped condition [19]). This affects the numerical damping of the analysis, which is the capability of some time-integration methods to eliminate additional erroneous oscillations induced by discretization in space [33, 36, 62]. Therefore, linear-viscous damping affects numerical damping, and in setting the details of an arbitrary analysis, for providing the required numerical damping, attention to linear-viscous damping is essential. In view of the objective of this paper, further discussion on numerical damping is left for future works.

4. Generalization

In the discussion presented in Section 2, the damping was assumed linear, viscous, and classical (for MDOF systems [12, 19]). This is an assumption conventional in practice [12, 19, 20, 35, 44]), and in view of it, the damping force can be defined as (see eq. (4)):

$$\mathbf{f}_d = \mathbf{C}\dot{\mathbf{u}} \tag{27}$$

The discussion and the resulting achievements may however be also valid for other types of damping (see [73]), e.g.

$$\mathbf{f}_d = \mathbf{C}\dot{\mathbf{u}}^{\Gamma} \quad , \quad \Gamma \in Z^{+} \tag{28}$$

In a review on the discussion presented in Section 2, the nature and type of damping affects the presented discussion negligibly. In more detail, by replacing eqs. (16), (17), and (20), with eqs. (29)-(31), stated below:

$$\begin{aligned} &\mathbf{M}\ddot{\mathbf{u}} + \mathbf{f}_d + \mathbf{f}_s = \mathbf{f}(t) \quad , \quad 0 \le t < t_{end} \\ &\mathbf{u}(t=0) = \mathbf{u}_0 \ , \ \dot{\mathbf{u}}(t=0) = \dot{\mathbf{u}}_0 \end{aligned} \tag{29}$$

$$\mathbf{f}_d \neq \overline{\mathbf{O}} \tag{30}$$

$$\begin{aligned} &\mathbf{M}\ddot{\mathbf{u}} + \mathbf{f}_s = \mathbf{f}(t) - \kappa \mathbf{f}_d^{\,a} \quad , \quad 0 \le t < t'_{end} \\ &\mathbf{u}(t=0) = \mathbf{u}_0 \ , \ \dot{\mathbf{u}}(t=0) = \dot{\mathbf{u}}_0 \end{aligned} \tag{31}$$

the discussion presented in Section 2 can be repeated and lead to similar results, if the probable nonlinearities in the definition of the damping force are modeled with negligible errors; see [74-76]. The last point is essential to preserve the validity of eqs. (14) and (15), resulted from eqs. (10)-(13), considering that eqs. (10)-(13) are valid for linear analyses [31, 33]. The specific consequence is that arbitrary physical damping would assist the numerical stability, provided the conditions below are met:

- The integration method is consistent.
- The damping and excitation contribute the integration scheme such that a constant value or matrix can be assigned to κ leading to identical responses for eqs. (29) and (31), when analyzed with the same integration step.
- The probable nonlinearities in the definition of physical damping are modeled with sufficient accuracy.
- The structural system is physically stable.

The difference between Figs. 2 and 3 from the points of view of computational effort and ease, and the benefits of the general rule claimed in this paper may increase for physical damping other than linear-viscous damping. The amount of the benefit depends directly on the number of coefficients defining the damping, e.g. equal to one (ξ) for linear-viscous damping. This highlights the significance of the achievements in this paper.

5. Discussion

The achievements attained in this paper, specifically maintaining a general rule for the influence of physical damping on numerical stability of time integration analyses, are important, because:

- The reduction of the computational effort associated with the study of numerical stability is considerable; see Figs. 2 and 3 and the brief discussion in the ending lines of Section 4.
- Research on new time integration methods is in rapid progress (see Table 3 and [4-18, 77]). Accordingly, study on the features and properties of new methods, e.g. numerical stability, would rather be facilitated. The main achievement in this paper is a step to materializing this objective; see Figs. 2 and 3 and [48].

Table 3. Number of researches with "new time integration method" in the body of the research manuscript according to Google Scholar search.

Years	1983-1987	1988-1992	1993-1997	1998-2002	2003-2007	2008-2012	2013-2017
Number	0	4	11	17	12	19	38

- The conditions discussed in Sections 2 and 4 can simply be tested. Accordingly, the achievements can simply be implemented in practice.
- When the conditions stated in Sections 2 and 4 are satisfied, there exists an amount of linear-viscous damping that can stabilize arbitrary unstable analysis.
- The discussion presented in Sections 2-4 takes into account all step-by step time integration methods, for which eq. (10) can be derived. Equation (10) and amplification matrix are conceptually equivalent to the nature of step-by-step solution of second order ordinary initial value problems [20, 31, 33, 48]. Consequently, the presented discussion includes not only single-stage implicit or explicit methods [31, 33], but also different predictor-corrector and multi-stage methods, e.g. see [31, 78, 79].

Furthermore, in the study of new time integration methods, it is conventional to consider the requirements derived for the numerical stability of linear analysis as necessary conditions for the numerical stability of nonlinear analyses; e.g. see [12, 33, 69, 75]. No new time integration method is introduced in this paper, and time integration methods are specifically important in nonlinear analysis. Considering these, in view of the discussion presented in Section 2, the achievements can be valid for nonlinear analysis, when the nonlinearity is via the internal force (see eq. 1) and

$$\mathbf{f}_{\text{int}} = \mathbf{f}_s + \mathbf{f}_d \tag{32}$$

($\mathbf{f}_s$ represents the internal forces in the structural system originated in the relative displacement of different parts of the system, and $\mathbf{f}_d$ stands for the internal forces resisting against motion; see also eq. (27)), provided nonlinearity iterations are sufficiently strict; see [76]. Figures 20-22 address an example.

Loosening the conditions restricting the achievements of this paper, i.e. the four conditions stated in the ending part of Section 4, is a major area for further research. Such studies may lead to elimination of physical damping from the study of numerical stability (of time integration methods). Even more, in long term, the importance of damping may disappear from the study of many time integration methods.

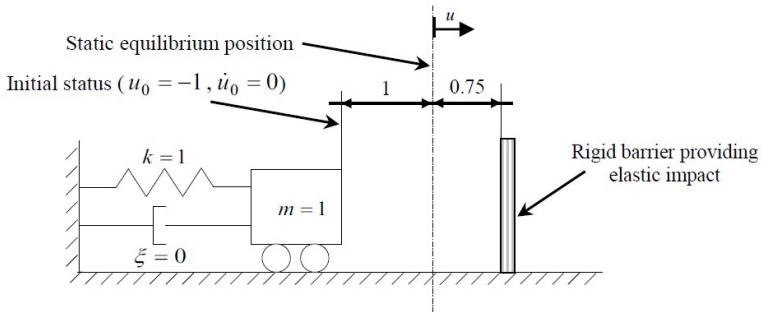

Fig. 20. Initial status and details of a free vibration nonlinear SDOF system to study the influence of viscous damping on numerical stability.

6. Conclusions

In time integration analysis of the semi-discretized equation of motion below:

$$\begin{aligned} &\mathbf{M}\ddot{\mathbf{u}} + \mathbf{f}_{\text{int}} = \mathbf{f}(t) \quad , \quad 0 \le t < t_{end} \\ &\mathbf{f}_{\text{int}} = \mathbf{f}_s + \mathbf{f}_d \quad \left(\mathbf{f}_d \ne \bar{\mathbf{O}}\right) \\ &\mathbf{u}(t=0) = \mathbf{u}_0 \ , \ \dot{\mathbf{u}}(t=0) = \dot{\mathbf{u}}_0 \ , \ \mathbf{f}_{\text{int}}(t=0) = \mathbf{f}_{\text{int}_0} \\ &\mathbf{Q} \le \bar{\mathbf{O}} \end{aligned} \tag{33}$$

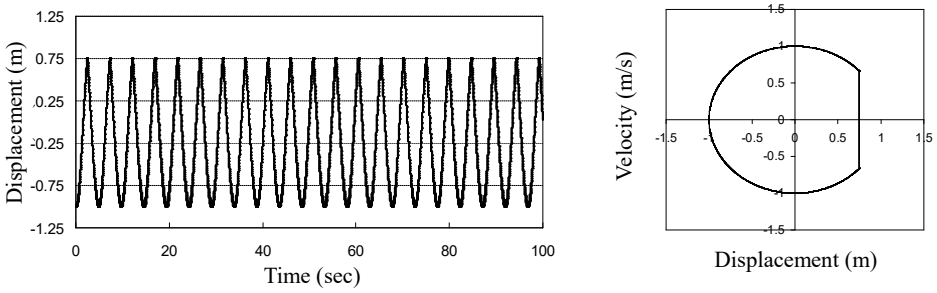

Fig. 21. Exact response of the system introduced in Fig. 20 displaying the physical stability of the nonlinear behavior: (a) Displacement history, (b) Plot of velocity versus displacement.

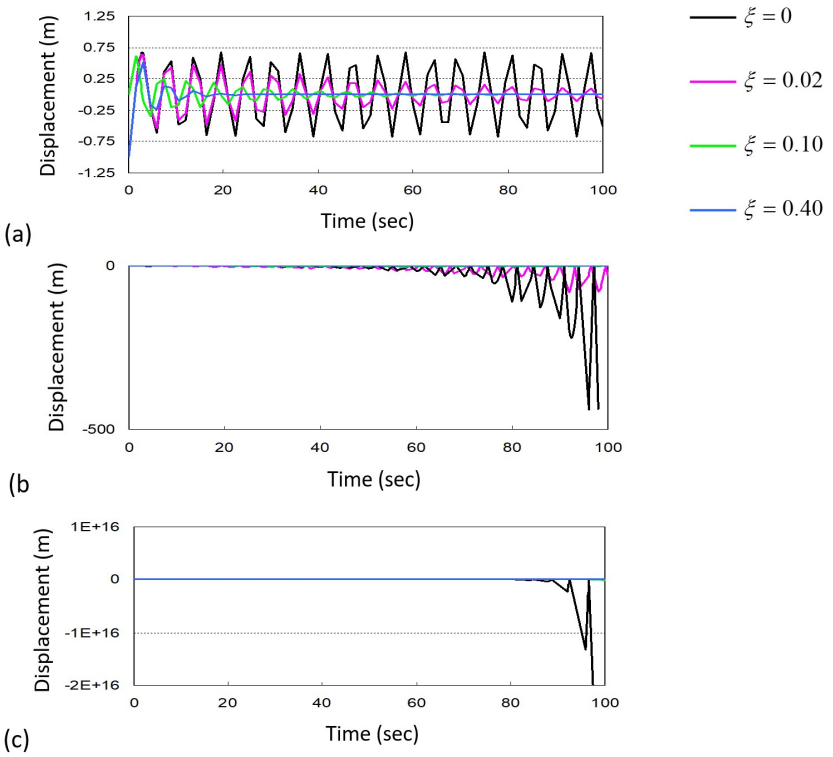

Fig. 22. Influence of linear-viscous damping on central difference analysis [64] of the system displayed in Fig. 20 when the nonlinearity modeling is controlled strictly: (a) $\Delta t = 1.5\,\mathrm{s}$, (b) $\Delta t = 2\,\mathrm{s}$, (c) $\Delta t = 4\,\mathrm{s}$.

the physical damping, $\mathbf{f}_d$, can be disregarded in the study of numerical stability, if

- The integration scheme is consistent.
- The damping and excitation appear in the time integration scheme such that, by adequate selection of κ, eqs. (16) and (20) (or eqs. (29) and (31)) can be modeled identically by the integration method.
- The residuals of the nonlinearity iterations are negligible.
- The behavior of the structural system is physically stable.

For linear-viscous damped systems, the above-mentioned achievement leads to Fig. 5. In addition, when the above four conditions are satisfied,

- For extremely high linear-viscous damping, the analysis becomes unconditionally stable.
- The influence of linear-viscous damping on numerical damping is different for different amounts of linear-viscous damping. Accordingly, in setting the details of time integrations methods, for eliminating the higher erroneous modes, physical damping should be taken into account.

Acknowledgement

The gratitude of the author is first to the reviewers of the paper, who have indirectly enhanced the paper by their comments. The author is also sincerely thankful to the editorial office of the prestigious Journal of Applied and Computational Mechanics (JACM), especially for their nice work in the typesetting stage. Finally, the last but not the least thanks of the author are to the managing editor of the JACM, Dr. Hamid M. Sedighi, for his collaboration guidance and patience.

Conflict of Interest

The authors declare no conflict of interest.

References

[1] IBC. *International Building Code*, International Code Council, USA, 2003.
[2] Hart, G.C., Jain, A., Performance-based wind evaluation and strengthening of existing tall concrete buildings in the Los Angeles region: dampers, nonlinear time history analysis and structural reliability, *Struct. Des. Tall Spec.* 23(16), 2014 1256-1274.
[3] Sassi, M.A., *Nonlinear Dynamic Analysis of Wind Turbine Towers Subject to Design Wind and Seismic Loads*, PhD Thesis, Colorado School of Mines, USA, 2016.
[4] Betsch, P., Steinmann, P., Inherently energy conserving time finite elements for classical mechanics, *J. Comput. Phys.* 160(1), 2000, 88-116.
[5] Bruels, O., Golinval, J.C., The generalized-α method in mechatronic applications, *Z. Angew. Math. Mech.* 86(10), 2006, 748-758.
[6] Eggl, S., Dvorak, R., An introduction to common numerical integration codes used in dynamical astronomy. *In The Dynamics of Small Solar System Bodies and Exoplanets*, Springer, USA, 2010, 431-480.
[7] Faragó, I., Havasi, Á., Zlatev, Z. (Eds.) *Advanced Numerical Methods for Complex Environmental Models: Needs and Availability*, Bentham Science Publishers, ebook, 2013.
[8] Kontoe, S., Zdrakovic, L., Potts, D.M., An assessment of time integration schemes for dynamic geotechnical problems, *Comput. Geotech.* 35(2), 2008, 253–264.
[9] Kpodzo, K., Fourment, L., Lasne P., Montmotonnet, P., An accurate time integration scheme for arbitrary rotation motion: application to metal forming formulation, *Int. J. Mater. Form.* 9(1), 2016, 71-84.
[10] Lemieux, J.F, Knoll, D.A., Losch, M., Girard, C., A second-order accurate in time IMplicit–EXplicit (IMEX) integration scheme for sea ice dynamics, *J. Comput. Phys.* 263, 2014, 375-392.
[11] Meijaard, J.P., Efficient numerical integration of the equations of motion of non-smooth mechanical systems, *Z. Angew. Math. Mech.* 77(6), 1997, 419-427.
[12] Paultre, P., *Dynamics of Structures*, John Wiley & Sons, USA, 2010.
[13] Soroushian, A., Integration step size and its adequate selection in analysis of structural systems against earthquakes. *In The Computational Methods in Earthquake Engineering*, Vol. 3, Springer, Norway, 2017, 285-328.
[14] Tamma, K.K. and D'Costa, J.F., A new explicit variable time-integration self-starting methodology for computational structural dynamics, *Int. J. Numer. Meth. Eng.* 33(6), 1992, 1165-1180.
[15] Kadioglu, S.Y., and Knoll, D.A., A fully second order implicit/explicit time integration technique for hydrodynamics plus nonlinear heat conduction problems, *J. Comput. Phys.* 229(9), 2010, 3237-3249.
[16] Bonelli, A., Bursi O. S., Generalized-α methods for seismic structural testing, *Earthq. Eng. Struct. D.* 33(10) 1067-1102.
[17] Yousuf, M., High-order time stepping scheme for pricing American option under Bates model, *Int. J. Comput. Math.* 96(1), 2019, 18-32.
[18] Ghasemi, M., Sonner, S. Eberl, HY. J., Time adaptive numerical solution of a highly non-linear degenerate cross-diffusion system arising in multi-species biofilm modeling, *Eur. J. Appl. Math.* 29(6), 2018, 1035-1061.
[19] Clough, R. W. Penzien, J., *Dynamics of Structures*, McGraw Hill, Singapore, 1993.
[20] Geradin, M., Rixen, D.J., *Mechanical Vibrations: Theory and Applications to Structural Dynamics*, John Wiley & Sons, USA, 2015.
[21] Gavin, H., *Structural Dynamics*, Duke University, USA, Class Notes CE 283, 2001.
[22] Hughes, T.J. R., Pister, K.S., Taylor R.L., Implicit-explicit finite elements in nonlinear transient analysis, *Comput. Methods Appl. Mech. Eng.* 17/18(1), 1979, 159–182.
[23] Wriggers, P., *Computational Contact Mechanics*, John Wiley & Sons, New York, 2002.
[24] Gear, C.W., *Numerical Initial Value Problems in Ordinary Differential Equations*, Prentice-Hall, NJ, 1971.
[25] Soroushian, A., Wriggers, P., Farjoodi, J., Asymptotic upperbounds for the errors of Richardson Extrapolation with practical application in approximate computations, *Int. J. Numer. Meth. Eng.* 80(5), 2009, 565–595.
[26] Henrici, P., *Discrete Variable Methods in Ordinary Differential Equations*, Prentice-Hall, NJ, 1962.
[27] Strikwerda, J.C., *Finite Difference Schemes and Partial Differential Equations*, Wadsworth & Books/Cole, Pacific Grove, CA, 1989.
[28] Richtmyer, R.D., Morton, K.W., *Difference Methods for Initial-value Problems*, Interscience Publishers, USA, 1967.
[29] Bathe, K.J., Wilson E.L., Stability and accuracy analysis of direct integration methods, *Earthq. Eng. Struct. D.* 1(3), 1972, 283-291.
[30] Lax, P.D., Richtmyer, R.D., Survey of the stability of linear finite difference equations, *Commun. Pur. Appl. Math.* 9(2), 1956, 267-293.
[31] Wood, W.L., *Practical Time Stepping Schemes*, Oxford, New York, 1990.
[32] Greenberg, M.G., *Advanced Engineering Mathematics*, Prentice-Hall, New Jersey, 1998.
[33] Belytschko, T., Hughes, T.J.R., (Eds.) *Computational Methods for Transient Analysis*, Elsevier, The Netherlands, 1983.
[34] Mengaldo, G., Wyszogrodzki, A., Diamantakis M., Lock, S. J. Giraldo F. X. and Wedi, N. P. Current and emerging time-integration strategies in global numerical weather and climate prediction, *Arch. Comput. Methods Eng.* 1-22, 2018.

[35] NZS 1170, *Structural Design Actions, Part 5: Earthquake Actions-New Zealand*, New Zealand, 2004.
[36] Hughes, T.J.R., *The Finite Element Method: Linear Static and Dynamic Finite Element Analysis*, Prentice-Hall, NJ, 1987.
[37] Soroushian, A., Wriggers, P., Farjoodi, J., Time integration of nonlinear equations of motion - numerical instability or numerical inconsistency? *In The Proc. 5th EUROMECH Nonlinear Oscillations Conference (ENOC 2005)*, European Mechanics Society, Eindhoven, The Netherlands, 2005.
[38] Han, B., Zdravkovic, L., Kontoe, S., Stability investigation of the Generalised-α time integration method for dynamic coupled consolidation analysis, *Comput. Geotech.* 64, 2015, 83-95.
[39] Rashidi, S., Saadeghvaziri M.A., Seismic modeling of multispan simply supported bridges using Adina, *Int. J. Comput. Struct.* 64(5–6), 1997, 1025–1039.
[40] Xie, Y.M., Steven, G. P., Instability, chaos, and growth and decay of energy of time-stepping schemes for nonlinear dynamic Equations, *Commun. Numer. Methods Eng.* 10(5), 1994, 393–401.
[41] Rose, I., Buffett, B., Heister, T., Stability and accuracy of free surface time integration in viscous flows, *Phys. Earth Planet. Inter.* 262, 2017, 90-100.
[42] Lee, K., A short note on time integration stability of dynamic frictional contact problems of elastic bodies, *P. I. Mech. Eng. K-J. Mul.* 230(2), 2016, 113-120.
[43] Cheng, M., Convergence and stability of step-by-step integration for model with negative-stiffness, *Earthq. Eng. Struct. D.* 16(2), 1988, 227-244.
[44] Elnashai, A.S., Sarno L.Di., *Fundamentals of Earthquake Engineering*, John Wiley & Sons, USA, 2008.
[45] Watkins, D. S., *Fundamentals of Matrix Computation* (2nd Ed.), John Wiley & Sons, USA, 2002.
[46] Houbolt, J. C., A recurrence matrix solution for the dynamic response of elastic aircraft, *J. Aeronaut. Sci.* 17(9), 1950, 540–550.
[47] Hart, G.C., Wong K., *Structural Dynamics for Structural Engineers*, John Wiley & Sons, USA, 1999.
[48] Soroushian, A., *Development of an Algorithm and Computer Program to Evaluate the Numerical Stability and Consistency of New Time Integration Methods*, International Institute of Earthquake Engineering and Seismology (IIEES), Iran, Report 7517, 2015. (in Persian)
[49] Piché, R., Nevalainen, P., Variable step Rosenbrock algorithm for transient response of damped structures, *P. I. Mech. Eng. C-J. Mec.* 213(2), 1998, 191-198.
[50] Zhu, M. Zhu, J.Q., Studies on stability of step-by-step methods under complex damping conditions, *J. Earthq. Eng. Eng. Vib.* 21(4), 2001, 59-62.
[51] Wang, J.T., Numerical stability of explicit finite element schemes for dynamic system with Rayleigh damping, *Earthq. Eng. Eng. Vib.* 22(6), 2002, 18-24.
[52] Wu, B., Bao, H., Ou., J., Tian, S., Stability and accuracy analysis of the central difference method for real-time substructure testing, *Earthquake Eng. Struct. Dyn.* 34(7), 2005, 705-718.
[53] Szabo, Z., Lukacs, A., Numerical stability analysis of a forced two-dof oscillator with bilinear damping, *J. Comput. Nonlin. Dyn.* 2(3), 2007, 211-217.
[54] Rezaiee-Pajand, M., Karimi-Rad, M., A new explicit time integration scheme for nonlinear dynamic analysis, *Int. J. Struct. Stab. Dyn.* 16(9), 2016, 1550054.
[55] Soroushian, A., A general rule for the effect of viscous damping on the numerical stability of time integration analyses. *In The Proc. 12th World Congress on Computational Mechanics and 6th Asia-Pacific Congress on Computational Mechanics (WCCM XII & APCOM VI)*, IACM, Seoul, South Korea, 2016.
[56] Soroushian, A., A general rule for the effect of arbitrary damping on the numerical stability of time integration analyses. *In The Proc., 7th International Conference on Computational Methods (ICCM2016)*, University of California at Berkeley, Berkeley, USA, 2016.
[57] Ding, Z., Li, L., Hu Y., A modified precise integration method for transient dynamic analysis in structural systems with multiple damping models, *Mech. Syst. Sig. Process*. 98, 2018, 613-633.
[58] Wood, W.L., On the effect of natural damping on the stability of a time-stepping scheme, *Commun. Appl. Numer. M.* 32(2), 1987, 141-144.
[59] Pourlatifi, S., *A method to distinguish numerical and physical instability in analysis of structural systems*, Msc Thesis, International Institute of Earthquake Engineering and Seismology, Iran, 2009.
[60] Zienkiewicz, O.C., Xie, Y.M., A simple error estimator and adaptive time stepping procedure for dynamic analysis, *Earthq. Eng. Struct. D.* 20(9) (1991) 871-887.
[61] Apostol, T.M., *Calculus*, Vol. I, John Wiley & Sons, New York, 1967.
[62] Kardestuncer, H., *Finite Element Handbook*, McGraw Hill, USA, 1987.
[63] Newmark, N.M., A method of computation for structural dynamics, *J. Eng. Mech.* 85(3), 1959, 67–94.
[64] Clough, R.W., *Numerical integration of equations of motion.* In The Lectures on Finite Element Methods in Continuum Mechanics, Univ. of Alabama, Tuscaloosa, AL, 1973, 525-533.
[65] Chung, J., Hulbert, G.M., A time integration algorithm for structural dynamics with improved numerical dissipation: The generalized-a method, *J. Appl. Mech.* 60(2), 1993, 371–375.
[66] Wilson, E.L. , *A Computer Program for the Dynamic Stress Analysis of Underground Structures*, University of California, Berkeley, Report 68-1,1968.
[67] Hilber, H.M., Hughes, T.J.R., Taylor R.L., Improved numerical dissipation for time integration algorithms in structural dynamics, *Earthq. Eng. Struct. D.* 5(3), 1977, 283–292.

[68] Hoff, C., Pahl, P.J., Development of an implicit method with numerical dissipation from a generalized single-step algorithm for structural dynamics, *Comput. Methods Appl. Mech. Eng.* 67(3), 1988, 367-385.
[69] Bathe, K.J., Conserving energy and momentum in nonlinear dynamics: a simple implicit time integration scheme, Int. J. Comput. Struct. 85(7-8), 2007, 437-445.
[70] Bathe, K.J., Noh, G., Insight into an implicit time integration scheme for structural dynamics, *Int. J. Comput. Struct.* 98-99(1), 2012, 1-6.
[71] Katsikadelis, J.T., A new direct time integration method for the equations of motion in structural dynamics, *Z. Angew. Math. Mech.* 94(9), 2014, 757-774.
[72] Rezaiee-Pajand, M., Karimi-Rad, M., A family of second-order fully explicit time integration schemes, *Comp. Appl. Math.* 37(3), 2017, 3431-3454.
[73] Lazan, B.J., *Damping of Materials and Members in Structural Mechanics*, Pergamon Press, UK, 1968.
[74] Allgower, E.L., Georg, K., *Numerical Continuation Methods, An Introduction*, Springer, New York, 1980.
[75] Kuhl D., Crisfield M.A., Energy-conserving and decaying algorithms in non-linear structural dynamics, *Int. J. Numer. Meth. Eng.* 45(5), 1999, 569–599.
[76] Soroushian, A., Wriggers, P., Farjoodi, J., Practical integration of semi-discretized nonlinear equations of motion: proper convergence for systems with piecewise linear behaviour, *J. Eng. Mech.*, 139(2), 2013, 114-145.
[77] Soroushian, A., Farjoodi, J., Bargi, K., Rajabi, M., Saaed, A., Arghavani, M., Sharifpour, M.M., Two versions of the Wilson-θ time integration method. *In The Proc. 10th International Conference on Vibration Problems (ICOVP 2011)*, Prague, Czech Republic, 2011.
[78] Rezaiee-Pajand, M. Karimi-Rad, M., An accurate predictor-corrector time integration method for structural dynamics, *Int. J. Steel Struct.*, 17(3), 2017, 1033-1047.
[79] Rio G., Soive A. Grolleau V., Comparative study of numerical explicit time integration algorithms, *Adv. Eng. Software* 36(4), 2005, 252-265.